

SIMULATION OF SPACE RADIATION DOSES ON NANO-SATELLITES IN EARTH ORBIT*

M.F. TRUSCULESCU^{1,2}, O. SIMA²

¹*Institute for Space Sciences, Magurele, Romania, marius.trusculescu@spacescience.ro*

²*Faculty of Physics, University of Bucharest, Magurele, Romania, octavian.sima@ik.fzk.de*

(Received September 30, 2009)

Abstract. This paper analyzes space radiation effects for Goliat - a typical 100 mm nano-satellite on Low Earth Orbit. Using estimated flux data as input, the effects were investigated by means of Monte Carlo simulations. The nano-satellite model was integrated with the GEANT 3.21 code for estimating the received radiation dose.

Key words: space radiation, radiation effects, Monte Carlo simulation, space, satellites, cosmic particles.

1. INTRODUCTION

The nano-satellite class of less than 10 kilograms spacecrafts is a recent and rapid development in the space industry. Using off the shelf components, design and manufacturing costs are considerably decreased. As a consequence, reliability needs to be maintained by precisely taking into account the harmful agents of the space environment.

This paper presents the work done into modeling the radiation environment effects for a typical small size satellite from the CubeSat class. Evolved in last decade, the model standardizes a cubic shaped satellite measuring 100 mm on each side and with a weight of maximum 1 kilogram.

2. MODEL

The model required for the simulation has two components: the radiation environment and the spacecraft. Both of them are modeled for a specific nano-satellite mission.

* Paper presented at the Annual Scientific Session of Faculty of Physics, University of Bucharest, June 5, 2009, Bucharest-Măgurele, Romania.

2.1. RADIATION ENVIRONMENT

Estimates on the particles fluxes interacting with the satellite have to take into account the characteristics of the three important radiation sources on Earth orbit: the Sun, trapped radiation regions near the planet, galactic and intergalactic cosmic rays [1, 2, 3].

Having a cyclic activity (approx.11 years), the Sun sources mainly protons and alpha particles with some minor heavy ions contributions in the radiation flux. An important characteristic of the Sun generated particles is that their flux has a cut-of energy, above which it decreases to values close to zero.

Trapped radiation regions are areas in Earth's magnetosphere where certain charged particles are constrained on a cyclic trajectory around planetary magnetic lines of force. There are two important such regions, the Inner and the Outer Van Allen Belt formed by protons, respectively electrons.

Known as Galactic Cosmic Rays, particles produced and accelerated outside the Solar System, mainly fully ionized elements arrive near Earth at fluxes dependant on solar activity. Unlike particles coming from the Sun, Galactic Cosmic Rays have non zero fluences for extremely high energies (particles above $>1\text{GeV/nucleon}$ have contributions that can't be neglected).

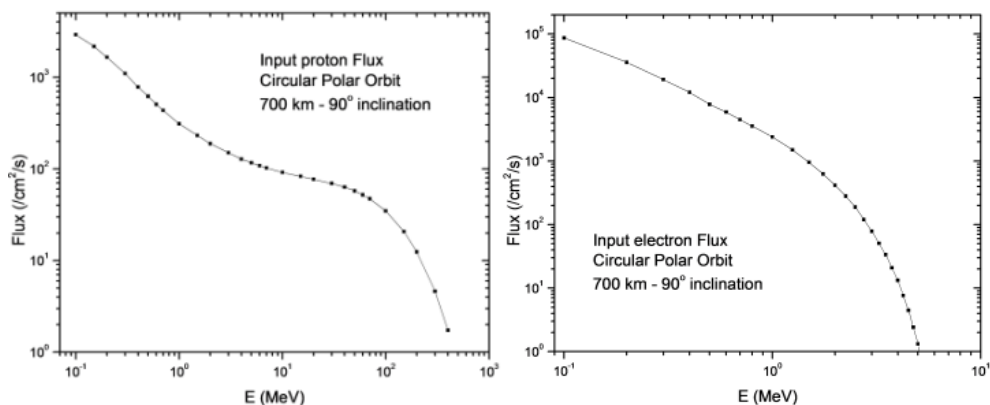


Fig. 1 – Proton flux (left panel) and electron flux (right panel) used in simulations.

Of most importance when trying to estimate the radiation flux is the time in the solar cycle when the analysis is conducted. More important though is the orbit of the satellite as the radiation environment varies greatly with both altitude and inclination.

For the purpose of this simulation the radiation environment has been estimated for a circular polar orbit at 700 km altitude (Fig. 1). The orbit was selected due to the high rate of occurrence for the studied satellite class. The fluxes for the radiation environment for all the particles and sources studied have been estimated using two online simulation tools: CRÈME96 Online [4] and Spenvis [5].

2.2. SPACECRAFT MODEL

A model of the satellite was integrated in the GEANT 3.21 program [6]. The spacecraft parametrization includes geometric and material models down to subsystem level for the spacecraft. An approximation, based on the satellite CAD design, was transferred to the geometry UGEOm subroutine.

The following subsystems were included in the model with their corresponding materials:

- STRUCT – (EXT) Aluminum mechanical structure of the satellite (Standard aluminum)
- OBC1 – main processor board including microcontroller, peripherals and SD card
- MHX – 2.4 GHz radio module
- UHF – low power radio module
- EPS – electronic power supply unit
- BAT1 – primary Li-Ion battery pack
- BAT2 – secondary Li-Ion battery pack
- CAM – camera interface board including magnetometer sensor
- DET – scintillator radiation detector
- DSP – digital signal processor controller for image processing
- OBCII – (OBC2, OBC3, OBC4) secondary processor unit including microcontroller, peripherals, GPS unit and two electronic controllers
- PHOTO – vOBV, hOBV and fOBV three geometric segments of the lens mount (glass lenses and aluminum external structure)

For each distinct subsystem a material was defined based on chemical composition and mass properties. In Table 1 the composition and density for the materials defining each subsystem is presented.

Table 1

Material definition table

	Material	C	F	Sn	Pb	Al	Si	O	Density (g/cm ³)
Z element		6	9	50	82	13	14	8	
A element		12.01	19.00	118.71	207.20	26.98	28.09	16.00	
Atomic ratio	OBC	0.20	0.20	0.09	0.06	0.10	0.25	0.10	2.5
Mass ratio		0.06	0.09	0.28	0.29	0.07	0.17	0.04	
Atomic ratio	MHX	0.15	0.15	0.09	0.06	0.25	0.25	0.05	2.7
Mass ratio		0.04	0.07	0.27	0.27	0.16	0.17	0.02	
Atomic ratio	UHF	0.23	0.23	0.09	0.06	0.05	0.25	0.10	2.3
Mass ratio		0.07	0.11	0.28	0.29	0.03	0.18	0.04	
Atomic ratio	EPS	0.25	0.25	0.09	0.06	0.05	0.25	0.05	2.2
Mass ratio		0.08	0.12	0.28	0.29	0.03	0.18	0.02	
Atomic ratio	CAM	0.20	0.20	0.06	0.04	0.05	0.35	0.10	2.3

Table 1 (continued)

Mass ratio		0.07	0.11	0.22	0.22	0.04	0.29	0.05	
Atomic ratio	OBCII	0.20	0.20	0.06	0.04	0.10	0.30	0.10	2.4
Mass ratio		0.07	0.11	0.22	0.23	0.08	0.25	0.05	
Atomic ratio	DSP	0.15	0.15	0.03	0.02	0.30	0.27	0.08	2.7
Mass ratio		0.06	0.10	0.13	0.13	0.28	0.26	0.04	
Atomic ratio	PHOTO	0.00	0.00	0.00	0.00	0.40	0.20	0.40	2.5
Mass ratio		0.00	0.00	0.00	0.00	0.47	0.25	0.28	

Material Aluminum and Vacuum are predefined in GEANT. Also the detector material (DET) was calculated as C_8H_8 (33%) and $C_{14}H_8O_2$ (67%) following the specifications of the manufacturer.

Radiation effects estimation uses dose for cumulative effects and linear energy transfer for single event effects caused by high energy particles [7, 8, 9].

3. SIMULATION ALGORITHM AND RESULTS

The program developed for the simulation is based on GEANT 3.21. The program is initialized by reading a two variable file in which the user must specify the number of initial particles – TRIG – and the particle type as GEANT a code number – TYPE – (E.g.: “3” for electron, “14” for proton).

It is in the initialization subroutine where data is read from the input energy file that was previously created from the flux estimates. The program needs input under the form of a four column ASCII file where the first column is the energy and the last is the probability of selection for that energy.

For each initial particle the program randomly chooses the initial energy in accordance with the probabilities from the flux input file. Isotropic radiation field is simulated by having the initial emission point evenly distributed on a spherical surface having its diameter equal to the satellite’s diagonal [10].

Each particle is transported towards the satellite and the energy lost in each step is counted for each material in a vector.

The developed program was initially run for trapped protons and electrons, which give the highest flux components on the chosen orbit. A number of $1E+06$ initial particles were simulated and the results are presented in Fig. 2.

As observed from Fig. 2 representations, the largest fraction of the proton energy deposition is retained by the mechanical structure, an order of magnitude above the other subsystems. When compared to other subsystems, all the onboard processors – OBC, OBCII and DSP – are susceptible to radiation induced effects.

For electron fluxes the structure receives energies more than two orders of magnitude above the other subsystem (not included in figure). One can observe that both on board computers (OBC and OBCII) receive important contributions of doses. Also in both the proton and electron case the estimate for the radiation detector is below most of the systems and a dose value measured at the detector

would be an underestimate of the real dose in the satellite. The absolute values of the doses are sensitive to the input flux values. However, the ratio of the doses received by different subsystems is less sensitive to the flux considered in simulations. Therefore reliable estimates of the dose in various subsystems can be obtained by multiplying the real dose recorded by the onboard radiation detector with the computed ratio of the corresponding dose. Thus, the simulation enables the identification of the dose in each of the satellite subsystems. Moreover it is possible to correlate computer errors with the momentary dose measurements, leading to better understanding of the radiation effects.

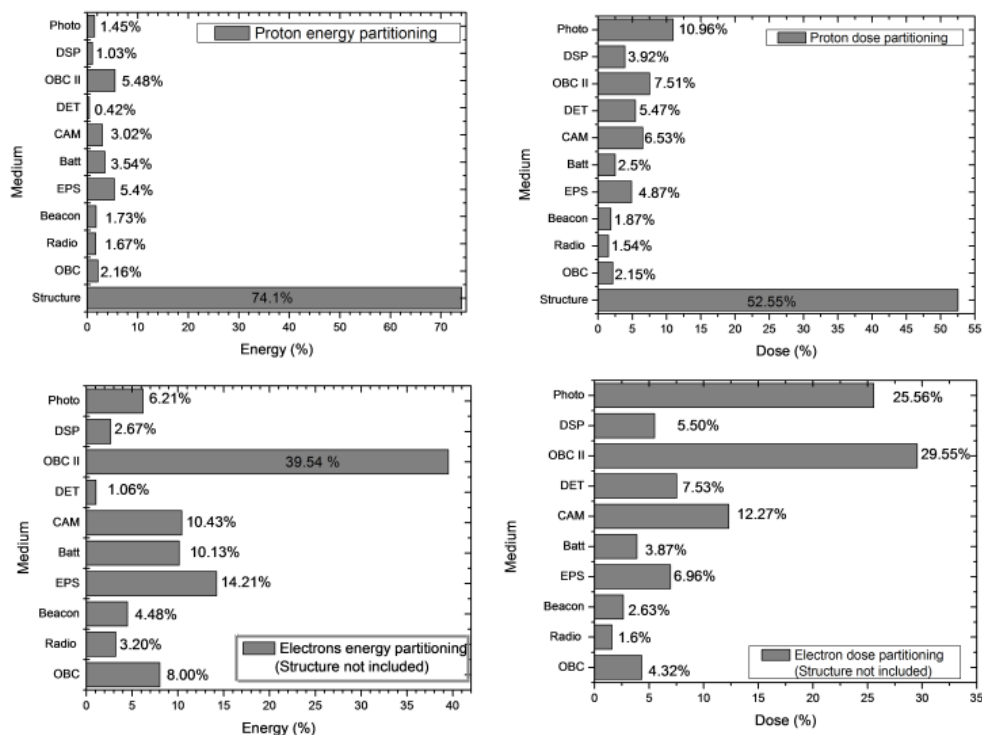


Fig. 2 – Average distribution of proton energy deposition (upper left panel), radiation dose (upper right panel) and electron energy deposition (lower left panel), radiation dose (lower right panel) for each satellite subsystem.

4. SUMMARY AND CONCLUSIONS

A GEANT 3.21 based program was written for the purpose of this research. The geometric and material models were created based on a real nano-satellite and the radiation environment was estimated for a typical orbit. Simulations were run repeatedly with the same conditions and energy deposited in each subsystem was

calculated. Based on this value the energy partitioning and dose partitioning for each subsystem were calculated.

Future work includes the analysis of single event effects through Linear Energy Transfer estimates and the elaboration of a more detailed geometric model. Once the satellite is in orbit and detector data is available, correlations will be made between the dose measurements and the performance of the on board subsystems.

REFERENCES

1. A.J. Tycal, J.H. Adams *et al.*, *CREME96: A Revision of the Cosmic Ray Effects on Micro-Electronics Code*, IEEE Transactions on Nuclear Science, **44**, 6, pp. 2150–2160, 1997.
2. J.H. Adams *et al.*, *Cosmic Ray Effects on Microelectronics, Part I*, NRL Memorandum Report, 4506, pp. 1–92, 1981.
3. J.H. Adams, *Cosmic Ray Effects on Microelectronics. Part IV*, NRL Memorandum Report, 5901, pp. 1–19, 1987.
4. *** <https://creme96.nrl.navy.mil/>.
5. *** <http://www.spennis.oma.be/>.
6. *** *GEANT Detector Description and Simulation Tool*, CERN Application Software Group CERN Program Library, W5013, pp. 1–465, 1994.
7. J. Barth, *Applying Computer Simulation Tools to Radiation Effects Problems – Section I Modelling Space Radiation Environments*, 1997, IEEE Nuclear and Space Radiation Conference, pp. 1–83.
8. C. Barnes, L. Selva, *Radiation Effects in MMIC Devices*, in S. Kayali, G. Ponchack, R. Shaw Eds., *GaAs MMIC Reliability Assurance Guideline for Space Applications*, JPL Publication, Pasadena USA, 1996, pp. 203–243.
9. A.J. Tylka *et al.*, *Single Event Upsets Caused by Solar Energetic Heavy Ions*, IEEE Transactions on Nuclear Science, **43**, 6, pp. 2758–2766, 1996.
10. O. Sima, *Simularea Monte-Carlo a transportului radiatiei*, Edit. All, Bucharest, Romania, 2004, pp. 1–188.